



UNIVERSITA' DI NAPOLI "FEDERICO II"

**DOTTORATO DI RICERCA
BIOCHIMICA E BIOLOGIA MOLECOLARE E CELLULARE
XXVIII CICLO**

**Novel small inhibitors targeting CDC25 dual specificity
phosphatases and displaying *in vitro* efficacy in melanoma cells**

Alessandra Capasso

Tutor
Prof. Emmanuele De Vendittis

Coordinator
Prof. Paolo Arcari

Co-Tutor
Prof. Maria Rosaria Ruocco

Academic Year 2014/2015

SUMMARY

CDC25 phosphatases are important regulators of several steps in the cell cycle, including the activation of various cyclin-dependent kinases (CDKs). They also play a role in the cellular response to DNA damage. Mammalian cells express three forms of CDC25: CDC25A, -B and -C. Overexpression of these phosphatases was reported in the development of several human malignancies, including melanoma. Therefore, CDC25 represent promising targets for anticancer drug discovery. Recently, the compound **NSC 119915** was identified as a new quinonoid CDC25 inhibitor with potent antiproliferative activity on cancer cells. In order to improve the inhibitory potency of this compound, 126 structurally related analogs were found by ligand-based chemoinformatic methods. Twenty-five of these structures were synthesized and analyzed by an *in vitro* assay to evaluate their inhibition properties on CDC25 phosphatases activity. Eight of these (**5-9**, **21**, **24**, and **25**) possessed high inhibitory activity towards CDC25A, -B and -C, and were tested in a cellular context using two human melanoma cell lines, A2058 and SAN. Only the compound **7** (cpd **7**) exerted a reduction of proliferative rate of both melanoma cell lines, arrested melanoma cells in G2/M, and caused a reduction of the protein levels of CDC25A and CDC25C. Furthermore, an intrinsic apoptotic pathway was induced, which was mediated by ROS, because it was reverted in the presence of antioxidant N-acetyl-cysteine (NAC). Finally, cpd **7** provoked a significant reduction of the Bcl-2/Bax ratio, decreased the protein levels of phosphorylated Akt and increased those of p53, thus contributing to the regulation of chemosensitivity through the control of downstream Akt pathways in melanoma cells. In conclusion, our data emphasize that CDC25 could be considered as a possible oncotarget in melanoma cells and that cpd **7** is a small CDC25 inhibitor that merits to be further evaluated as a chemotherapeutic agent for melanoma, likely in combination with other therapeutic compounds

RIASSUNTO

Le fosfatasi CDC25 sono enzimi coinvolti nella regolazione del ciclo cellulare che agiscono defosforilando ed attivando specifiche chinasi dipendenti da cicline (CDKs). Inoltre, CDC25 svolge un ruolo chiave nella modulazione della risposta cellulare al danno al DNA. Sono state identificate tre forme di CDC25: CDC25-A, -B e -C, ciascuna differentemente implicata nelle diverse fasi del ciclo cellulare. Un'elevata espressione di queste fosfatasi è stata riscontrata in numerose neoplasie, compreso il melanoma. Pertanto, tali enzimi sono considerati un possibile bersaglio molecolare nello sviluppo di nuove strategie terapeutiche antitumorali. Recentemente è stato identificato un nuovo inibitore di CDC25 a struttura chinonica, il composto NSC 119915. Allo scopo di approfondire lo studio sulle proprietà inibitrici di tale molecola, sono stati individuati attraverso studi chemoinformatici 126 analoghi di tale "lead compound". Tra questi, 25 composti sono stati sintetizzati e successivamente analizzati mediante dosaggi *in vitro*, per verificare il loro potenziale inibitorio sull'attività fosfataseica di CDC25. Solo 8 analoghi (**5-9**, **21**, **24** e **25**) mostravano un'elevata capacità inibitoria sulle tre forme di CDC25, e pertanto il loro potenziale effetto citotossico è stato valutato mediante studi biologici *in vitro*, utilizzando due linee cellulari di melanoma umano, A2058 e SAN. Tra gli 8 analoghi selezionati, solo il composto **7** induceva una significativa riduzione della capacità proliferativa di entrambe le linee di melanoma. In particolare, tale analogo provocava l'arresto delle cellule di melanoma in G2/M, causando una significativa riduzione dei livelli proteici di CDC25A e CDC25C. Inoltre, il composto **7** induceva un processo apoptotico intrinseco caspasi-dipendente, mediato da un incremento dei livelli intracellulari dei ROS. Infine, è stato osservato un effetto di tale composto su alcune vie di segnale che regolano processi di apoptosi, proliferazione e sopravvivenza cellulare. Infatti, nel corso del trattamento con il composto **7** è stata

evidenziata una marcata riduzione del rapporto Bcl-2/Bax, una riduzione dei livelli di pAkt ed un incremento di p53.

Nel complesso, questi dati suggeriscono che CDC25 potrebbe rappresentare un “oncotarget” nelle cellule di melanoma e che lo studio approfondito dei meccanismi coinvolti nei processi indotti dal composto **7** potrebbero contribuire a migliorare le prospettive terapeutiche di tale neoplasia, attraverso l'utilizzo combinato con altri farmaci chemioterapici.

Index

	Pag.
1. Introduction	1
2. Materials and Methods	5
2.1 <i>Materials and Reagentes</i>	5
2.2 <i>Database and chemoinformatic methods</i>	6
2.3 <i>In vitro assays of CDC25 phosphatase activity</i>	6
2.4 <i>Cell culture</i>	7
2.5 <i>3-(4,5-Dimethylthiazole-2-yl)-2,5-biphenyltetrazolium bromide (MTT) assay</i>	8
2.6 <i>Cell cycle analysis and evaluation of apoptosi</i>	8
2.7 <i>Measurements of caspase-3 and caspase-9 activity</i>	9
2.8 <i>Measurements of intracellular ROS content</i>	9
2.9 <i>Evaluation of mitochondrial membrane potential</i>	10
2.10 <i>Western blotting</i>	10
2.11 <i>Statistical analyses</i>	11
3. Results	
3.1 <i>Compound selection using chemoinformatics</i>	12
3.2 <i>Effect of the close analogs of NSC 119915on the phosphatase activity of purified recombinant forms of CDC25</i>	12
3.3 <i>Evaluation of CDC25 inhibitors on cell growth rate on A2058 and SAN cells</i>	18
3.4 <i>Effect of compound 7 on cell cycle progression and apoptosis</i>	20
3.5 <i>Effect of compound 7 on ROS generation and mitochondrial membrane potential</i>	26
3.6 <i>Effect of compound 7 on Akt activation and p53 protein levels</i>	31
4. Discussion/Conclusions	34

5. References	39
----------------------	----

List of Figure	
Figure 1. An overview of the regulatory function of CDC25s in cell cycle progression.	2
Figure 2. Known quinone-containing CDC25 Inhibitors.	3
Figure 3. Flow chart of the multiple ligand-based chemoinformatic strategy implemented in this work.	12
Figure 4. Effect of compound 7 on the Lineweaver-Burk plots of the A. CDC25A B. CDC25B and C. CDC25C phosphatase activity	16
Figure 5. Effects of NSC 119915 and its close analogs on cell growth rate of melanoma cells.	19
Figure 6. Effects of compound 7 on the distribution of cell cycle phases of A2058 cells.	20
Figure 7. Effects of compound 7 on the distribution of cell cycle phases of SAN cells.	21
Figure 8. Effect of compound 7 on CDC25A, B and C protein levels.	22
Figure 9. Effect of compound 7 on CDC25C protein levels.	23
Figure 10. Effect of compound 7 on the apoptosis of A2058 and SAN cells.	25
Figure 11. Effect of Z-VAD-FMK, a pan-caspase inhibitor, on the apoptotic process induced in melanoma cells by compound 7.	26
Figure 12. ROS production and their involvement in the apoptotic process of A2058 cells, as induced by treatment with compound 7.	27
Figure 13. ROS production and their involvement in the	28

apoptotic process of SAN cells, as induced by treatment with compound 7.

Figure 14. Effect of compound 7 on some apoptotic mitochondrial markers in A2058 cells. A. 30

Figure 15. Effect of compound 7 on some apoptotic mitochondrial markers in SAN cells. 31

Figure 16. Effect of compound 7 on pAkt and p53 protein levels. 33

List of Tables

Table 1. Compounds identified by multiple ligand-based chemoinformatic protocol	13
Table 2. Residual phosphatase activity of CDC25B in the presence of compound NSC 119915 or its 6-xanthone analogs	15
Table 3. Ki values of compound NSC 119915 or its 6-xanthone analogs towards CDC25A, -B and -C phosphatases	17

INTRODUCTION

Cell division cycle 25 proteins (CDC25s) are dual-specificity phosphatases (DSPs), that dephosphorylate conserved tyrosine and threonine residues of the cyclin-dependent kinases (CDKs) complexes; this event leads to the activation of these crucial regulators of the progression through the cell cycle [1,2]. Furthermore, CDC25s are key targets of checkpoint machinery, which is activated in response to DNA damage caused by UV light, ionizing irradiation, or chemicals. Therefore, the misregulation of these enzymes could be pivotal for causing genomic instability. There are three forms of CDC25 phosphatases in mammalian cells: CDC25A, -B, and -C [3]. CDC25A mainly controls G1/S progression, by dephosphorylating and activating the CDK4-cyclin D [4] and CDK6-cyclin D [5], as well as CDK2-Cyclin A and CDK2-Cyclin E complexes [6,7]. CDC25B and CDC25C are primarily required for the entry into mitosis. CDC25B is responsible for the initial activation of CDK1-Cyclin B complex at the centrosome during the G2/M transition, which is then followed by a complete activation of CDK1-cyclin B complexes by CDC25C in the nucleus at the onset of mitosis [8,9]. However, all three CDC25 forms are involved in the G1/S and G2/M transitions and in mitosis (Figure 1). CDC25 phosphatase activity is tightly regulated at transcriptional level and by multiple post-translational mechanisms such as inhibitory and activated phosphorylations, sub-cellular relocation and proteasome-mediated degradation [10], and by p53-dependent transcriptional repression [11,12]. The expression of CDC25A, CDC25B or both has been shown to be upregulated in a wide variety of human tumors, including melanoma [13]. With regard to CDC25C, only a few studies showed an overexpression of this form in tumours [14,15].

CDC25 overexpression can probably occur at different steps during tumorigenic pathway and contributes to the progression of the disease through a deregulation of the cell division cycle, cooperating with other

oncogenes involved in signalling pathway. Therefore, CDC25 phosphatases can represent ideal targets for the development of novel anticancer therapies [8].

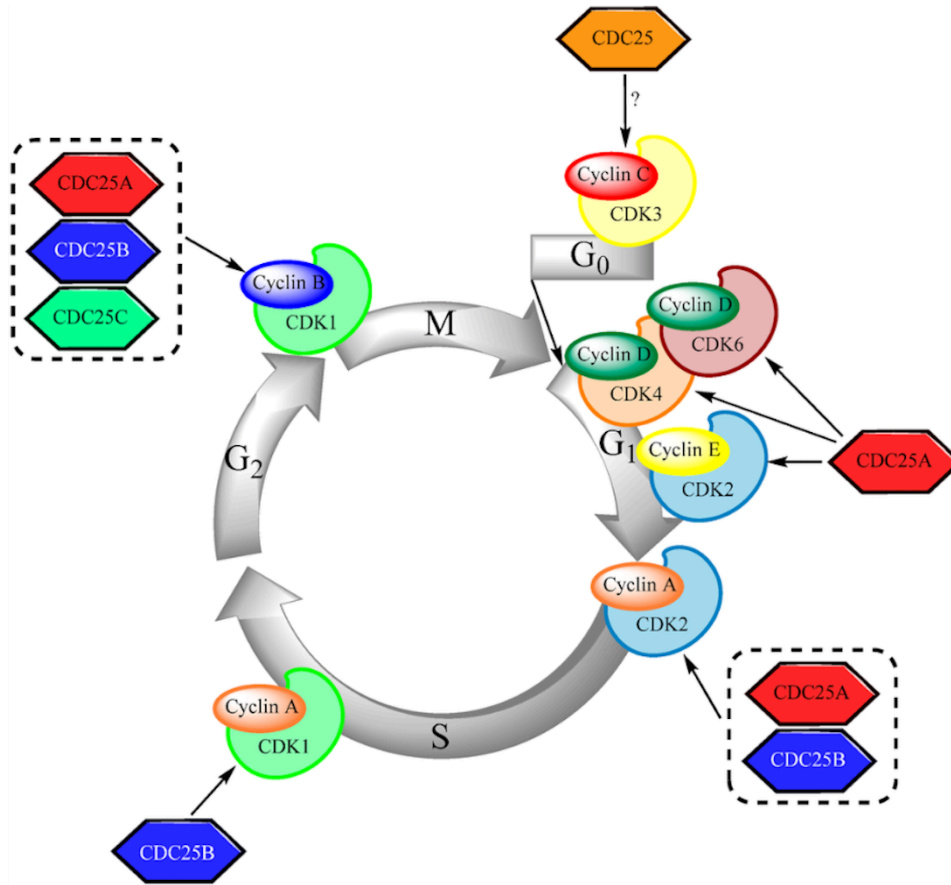


Figure 1. An overview of the regulatory function of CDC25s in cell cycle progression. At G₀-phase, cells that had been quiescent, re-enter the cell cycle after activation of CDK3/cyclin C. Dephosphorylation of CDK4/cyclin D, CDK6/cyclin D and CDK2 both in complex with cyclin E and cyclin A by CDC25s leads to the transition into the DNA-replication phase. At late S-phase, CDC25B activates CDK1/cyclin A. Finally, dephosphorylation of CDK1/cyclin B triggers mitotic entry, and in this important step all three CDC25 isoforms are involved. At the end of mitosis, both CDK1/cyclin B and the CDC25s are degraded and the cycle can start all over again.

A number of compounds, belonging to various chemical classes (phosphate bioisosteres, electrophilic entities, and quinone-based structures) have shown to possess an *in vitro* inhibitory power on CDC25 phosphatase activity. It is thought that there are three possible mechanisms through which these molecules may inhibit CDC25: reversible inhibition through binding to the active site of CDC25 [16,17], irreversible inhibition through a direct binding of the inhibitor to CDC25 [18,19], or oxidation of a critical cysteine residue (CX₅R) in the catalytic domain of these enzymes by reactive oxygen species (ROS) generated in cultured cells treated with quinone derivatives [20,21].

Many of the most potent CDC25 inhibitors are quinone-containing compounds, which inhibit *in vitro* all three forms of CDC25 in an unselective manner. Among these, **NSC 95397** [16], **NSC 663284** [18], **BN 82685** [22] and **IRC-083864** [23] are representative potent inhibitors (Figure 2). Recently, a new quinonoid CDC25 inhibitor, **NSC 119915**, has been discovered; this compound displayed irreversible inhibition, generated an increase of the intracellular ROS level, arrested cells in the G₀/G₁ and G₂/M phases of the cell cycle, and significantly suppressed the growth of human MCF-7 breast, PC-3 prostate, and K562 leukemia cancer cell lines [24].

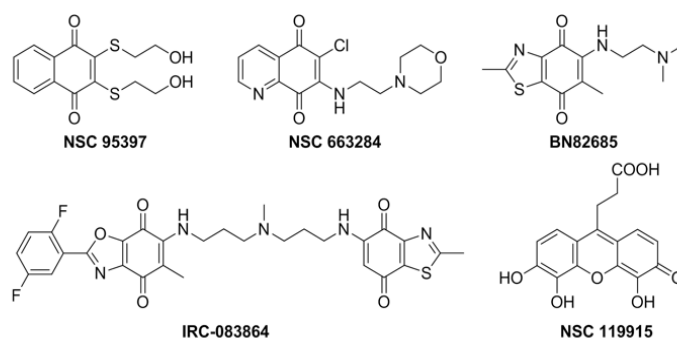


Figure 2: Known quinone-containing CDC25 Inhibitors.

It is known that malignant melanoma is an aggressive and deadly tumour with a high tendency to relapse and high metastasis rate. The development and progression of melanoma is often associated with alteration of some components of key signalling pathway that regulate proliferation, survival, growth factor receptor activation, differentiation, cell adhesion and migration. Hence, the discovery of new molecules acting through the modulation and inhibition of key pathways involved in cell proliferation and survival will be very helpful in the development of new therapeutic strategies against melanoma.

In this study, we characterized the inhibitory power of twenty-five analogs of **NSC 119915**. Among them, eight compounds, sharing the same 6-xanthone chemical motif (**5-9**, **21**, **24**, and **25**), exerted an *in vitro* inhibitory activity towards all three CDC25 forms, comparable with that shown by **NSC 119915**. We also investigated the cytotoxic effect of these molecules in a cellular context, using two melanoma cell lines, A2058 and SAN. The results indicated that only cpd **7** exerted a significant effect on the inhibition of cell proliferation, as revealed by the cytotoxicity tests. Furthermore, cpd **7** altered the cell cycle progression, modulated the CDC25 protein levels and caused the cell death, by inducing an apoptotic program, as evaluated through different markers. In addition, **7** induced an alteration of the cellular redox state and provoked a mitochondrial dysfunction, likely associated to the modulation of the pAkt and p53 protein levels.

2. MATERIALS AND METHODS

2.1 Materials and Reagents

Compounds, purchased from commercial vendors or kindly provided from the NCI/DTP, were dissolved in dimethyl sulfoxide (DMSO), and stock solutions at 10 mM concentration were prepared. Recombinant forms of the catalytic domains of CDC25A, -B and -C were obtained through the vectors pET28a-CDC25A-cd, pET28a-CDC25B-cd and pET28a-CDC25C-cd, kindly provided by H. Bhattacharjee (Florida International University, Herbert Wertheim College of Medicine, Miami, Florida), using the procedure already described [24]. The synthetic substrate for CDC25 phosphatase activity, 3-O-methylfluorescein phosphate (OMFP), was purchased from Sigma-Aldrich. Dulbecco's modified Eagle's medium (DMEM), Roswell Park Memorial Institute (RPMI) 1640 medium, fetal bovine serum (FBS), L-glutamine, penicillin G, streptomycin, and trypsin were purchased from Lonza (Milano, Italy). Propidium iodide (PI), dichlorofluorescein diacetate (DCFH-DA), Rhodamine 123 (R123), apocynin and N-acetyl-L-cysteine (NAC) were purchased from Sigma-Aldrich. A protease inhibitor cocktail was obtained from Roche Diagnostics S.p.A. (Monza, Italy). Caspase-3 and caspase-9 fluorimetric assay kits were purchased from BioVision (Milpitas, CA, USA). The pan-caspase inhibitor Z-VAD-FMK was purchased from Selleckchem (USA). Rabbit monoclonal antibody against glyceraldehyde 3-phosphate dehydrogenase (GAPDH) was obtained from Cell Signaling (Boston, MA, USA); mouse monoclonal antibody against CDC25A, CDC25C or Bcl-2, rabbit polyclonal antibody against CDC25B, pAkt or Bax, and each secondary antibody conjugated to horseradish peroxidase were obtained from Santa Cruz Biotechnology (Heidelberg, Germany). All other chemicals were of analytical grade and were purchased from Sigma-Aldrich.

2.2 Database and chemoinformatic methods

Chemoinformatic methods for the selection of 126 structurally related analogs of NSC 119915 were carried out in collaboration with the Department of Pharmacy, University of Naples Federico II. The NCI Open Database (<http://ntp.cancer.gov/>) was obtained from ZINC [25,26]. The compound database was processed with FILTER version 2.0.2 (OpenEye Scientific Software Inc., Santa Fe, USA, <http://www.eyesopen.com/>) to select a subset of lead-like compounds. The default parameters in the lead-like filter were used without further modifications. The resulting database was referred in this thesis as the NCI lead-like set.

2.3 In vitro assays of CDC25 phosphatase activity

The enzymatic activity of the catalytic domains of CDC25A, -B and -C were determined through a fluorimetric method, which monitored the dephosphorylation of the synthetic substrate OMFP, essentially as previously described [24]. In particular, the effect of the various inhibitors was first evaluated on the phosphatase activity of CDC25B in steady-state enzyme kinetic studies. To this aim, the activity of purified recombinant CDC25B was measured at 30°C in the presence of different concentrations of the various inhibitors, using a computer-assisted Cary Eclipse spectrofluorimeter (Varian) equipped with an electronic temperature controller. Excitation and emission wavelengths were set at 485 and 530 nm, respectively; both excitation and emission slits were set at 10 nm. The reaction mixture contained 10 nM CDC25B and different concentrations of the various inhibitors in 500 µL final volume of 20 mM Tris-HCl, pH 7.8, 1 mM dithiothreitol (DTT). DMSO was used as vehicle control. The reaction started with the addition of 25 µM OMFP, and the formation of the fluorescent product *o*-methylfluorescein was monitored continuously. The rate of OMFP hydrolysis was expressed as arbitrary units per min (a.u./min). The comparison of the rates determined in the

absence and in the presence of the various inhibitors allowed the calculation of the residual phosphatase activity, expressed as a percentage.

To measure the inhibition constant (K_i) of the recombinant forms of CDC25A, -B and -C towards the various inhibitors, the affinity of the different forms of CDC25 towards OMFP was measured either in the absence or in the presence of fixed concentrations of the various inhibitors. The reaction mixture contained 20 nM CDC25A, or 10 nM CDC25B, or 40 nM CDC25C, and different concentrations of the various inhibitors in 500 μ L final volume of 20 mM Tris-HCl, pH 7.8, 1 mM DTT. DMSO was used as vehicle control. The reaction started with the addition of 1–25 μ M OMFP, and the rate of OMFP hydrolysis was measured as indicated before. The corresponding Lineweaver-Burk plots allowed the calculation of the K_M for OMFP and of the maximal rate (V_{max}) of OMFP hydrolysis. In the presence of the various inhibitors the K_M for OMFP remained essentially unchanged, whereas the V_{max} decreased, thus indicating that the selected compounds were noncompetitive inhibitors of CDC25. The K_i values were obtained from the decrease of V_{max} in the presence of the inhibitor, according to the equation $V_{max}' = V_{max}/\{1+([I]/K_i)\}$, where V_{max}' represents the V_{max} measured in the presence of the concentration $[I]$ of the inhibitor. The K_i values were obtained from at least three independent experiments and reported as mean \pm S.E.

2.4 Cell culture

The human melanoma cell line A2058, kindly provided by CEINGE (Naples, Italy), and SAN cells [27] were derived from lymph nodal metastases and grown in DMEM and RPMI 1640, respectively, supplemented with 10% FBS, 2 mM L-glutamine, 100 IU/mL penicillin G, and 100 μ g/mL streptomycin in humidified incubator at 37°C under 5% CO₂ atmosphere. All cells were split and seeded every three days and

used during the exponential phase of growth. Cell treatments were always carried after 24 h from plating.

2.5 3-(4,5-Dimethylthiazole-2-yl)-2,5-biphenyltetrazolium bromide (MTT) assay

The MTT assay was used to detect cell proliferation essentially as previously described [28]. Briefly, A2058 and SAN cells were plated in 96-well microtiter plates (100 μ L/well) at 4000 and 6000 cells/well, respectively. After 24-h seeding, cells were treated with the selected compounds added at 25, 50 or 100 μ M concentration, or with 0.5% (v/v) DMSO as a vehicle control. After 24-h, 48-h or 72-h treatment, and upon the addition of 10 μ L of MTT solution in the dark, the plate was incubated for 3 h at 37°C under CO₂ atmosphere. After medium aspiration and solubilization of formazan crystals, absorbance was measured at 570 nm, using an ELISA plate reader (Bio-Rad, Milano, Italy).

2.6 Cell cycle analysis and evaluation of apoptosis

Cells were seeded into 6-well plates at 3×10^5 cells/well for 24 h at 37°C; after the addition of 100 μ M cpd **7** or 0.5% DMSO as a vehicle control, the incubation of treated cells continued for 16 or 24 h. After each treatment, cells were harvested with trypsin, centrifuged and the pellet was resuspended in phosphate-buffered saline (PBS). For cell cycle analysis, cells were fixed with 70% (v/v) cold ethanol and stored at –20°C for 1 h. Then, cells were washed with cold PBS, centrifuged and the pellets were resuspended in 200 μ L of a non-lysis solution containing 50 μ g/mL PI. For the evaluation of apoptosis, cells were not fixed in ethanol and directly resuspended in 200 μ L of a hypotonic lysis solution containing 50 μ g/mL PI. After incubation at 4°C for 30 min, cells were analyzed with a FACScan flow cytometer (Becton Dickinson) for

evaluating the distribution in cell cycle phases or the presence of nuclei with a DNA content lower than the diploid.

2.7 Measurements of caspase-3 and caspase-9 activity

To estimate caspase-3 and caspase-9 activity during the treatment with cpd **7**, the respective enzymatic activities were measured by using caspase-3 and caspase-9 fluorimetric assay kits, according to the manufacturer's protocol, essentially as previously described [29]. Briefly, cells were seeded into 75 cm² plates (2×10^6 cells/plate) for 24 h at 37°C and then treated with 100 µM **7** or 0.5% DMSO. At the end of each incubation, cells were collected, washed with PBS, and finally lysed at 4°C in the cell lysis buffer. Cell lysates were incubated with 50 µM DEVD-AFC or LEHD-AFC substrates at 37°C for 2 h, to detect caspase-3 or caspase-9 activity, respectively, using a Cary Eclipse fluorescence spectrophotometer (Varian). Excitation and emission wavelengths were set at 400 nm and 505 nm, respectively; both excitation and emission slits were set at 10 nm.

2.8 Measurement of intracellular ROS content

The intracellular ROS level was monitored using the oxidation-sensitive fluorescence probe DCFH-DA. Cells were seeded into 6-well-plates (3×10^5 cells/plate) for 24 h at 37°C and then treated at various times with 100 µM cpd **7** or 0.5 % DMSO. DCFH-DA was added in the dark at 10 µM final concentration 30-min before the end of each incubation; then, cells were collected, washed in PBS, and finally resuspended in 500 µL PBS for fluorimetric analysis. Measurements were realized in the above-mentioned fluorescence spectrophotometer; excitation and emission wavelengths were set at 485 nm and 530 nm, respectively; both excitation and emission slits were set at 10 nm. The effect of **7** on ROS production was also estimated after pretreatment of cells with 10 mM NAC for 1 h.

2.9 Evaluation of mitochondrial membrane potential

Mitochondrial membrane potential was evaluated by measuring the incorporation of the fluorescent probe R123, essentially as previously described [30]. Briefly, cells were seeded into 6-well-plates (3×10^5 cells/well) for 24 h at 37°C, and then incubated at 37°C for 1 h in the presence of 5 μ M R123, washed twice with PBS, and placed in medium containing 100 μ M cpd **7** or 0.5% DMSO. After various times from treatment, cells were harvested, washed and centrifuged for 10 min at 4°C. The cellular pellet was resuspended in 500 μ L PBS. The fluorescence of cell-associated R123 was detected in the above-mentioned fluorescence spectrophotometer, using excitation and emission wavelengths of 490 and 520 nm, respectively; both excitation and emission slits were set at 10 nm.

2.10 Western blotting

A2058 cells were seeded into 6-well-plates (3×10^5 cells/plate) for 24 h at 37°C and then treated at different times with 100 μ M cpd **7** or 0.5% DMSO. After treatment, cells were harvested, washed with PBS and then lysed in ice-cold modified radio immunoprecipitation assay (RIPA) buffer (50 mM Tris-HCl, pH 7.4, 150 mM NaCl, 1% Nonidet P-40, 0.25% sodium deoxycholate, 1 mM Na_3VO_4 and 1 mM NaF), supplemented with protease inhibitors and incubated for 30 min on ice. The supernatant obtained after centrifugation at 12,000 rpm for 30 min at 4°C constituted the total protein extract. The protein concentration was determined by the method of Bradford, using bovine serum albumin as standard [31]. Equal amounts of total protein extracts were used for Western blotting analysis. Briefly, protein samples were dissolved in SDS-reducing loading buffer, run on 12% SDS/PAGE and then transferred to Immobilon P membrane (Millipore). The filter was incubated with the specific primary antibody at 4°C overnight and then with the secondary antibody at room temperature for 1 h. Membranes were then analysed with an enhanced

chemiluminescence reaction, using Super Signal West Pico kit (Pierce) according to manufacturer's instructions; signals were visualized by autoradiography.

2.11 Statistical analysis

Data are reported as average and standard error. The statistical significance of differences among groups was evaluated using ANOVA, with the Bonferroni correction as post hoc test or the Student *t* test where appropriate. The significance was accepted at the level of $p < 0.05$.

3. RESULTS

3.1 Compound selection using chemoinformatics

The present work was aimed at the identification of novel structural analogs with increased CDC25 inhibition power compared to the lead compound **NSC 119915**. To this aim, a database of compound structures from ZINC drug-like library and NCI lead-like set was used in collaboration with the Department of Pharmacy, University of Naples Federico II. After combination of the results obtained with these databases, and elimination of duplicate structures, a total of 126 unique compounds were identified, that were predicted to be similar in some way to the lead compound **NSC 119915** by one or more methods (Figure 3).

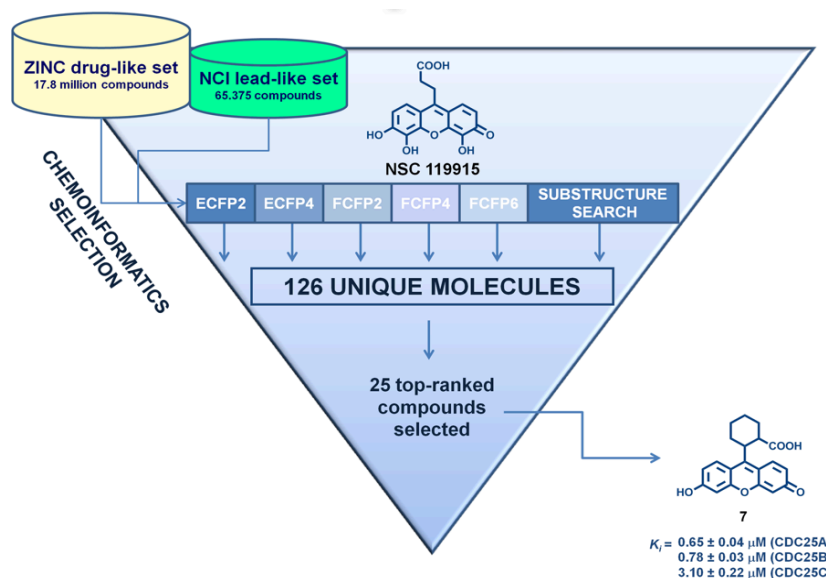
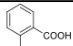
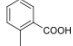
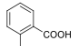
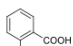
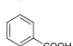
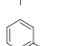
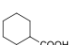
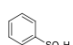
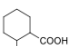
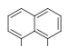
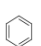
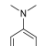
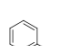
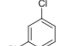
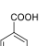
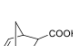
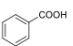
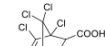
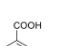


Figure 3: Flow chart of the multiple ligand-based chemoinformatic strategy implemented in this work.

To avoid an extensive and time-consuming screening of such a great number of compounds by *in vitro* assays, top-ranked 25 compounds were selected, and purchased or requested from the NCI Developmental

Therapeutics Program (DTP) (Table 1).

Table 1: Compounds identified by multiple ligand-based chemoinformatic protocol

Cpd	Code	R ₁	R ₂	R ₃	R ₄	R ₅	Cpd	Code	R ₁	R ₂	R ₃	R ₄	R ₅
1	NSC 158113	CH ₃	H	H	H	H	14	NSC 4202		H	I	I	H
2	ZINC 04015433	CH ₃	OH	H	H	OH	15	NSC 4905		I	I	I	I
3	NSC 158115	COOH	H	H	H	H	16	ZINC 04409973		H	Cl	Cl	H
4	NSC 158112	CH ₂ CH ₂ COOH	H	H	H	H	17	ZINC 04352921		H	Br	Br	H
5	NSC 119894	CH=CHCOOH	H	H	H	H	18	NSC 2087		Br	Br	Br	Br
6	NSC 119911	CH=CHCOOH	H	OH	OH	H	19	ZINC 04261930		NO ₂	Br	Br	NO ₂
7	NSC 119892		H	H	H	H	20	ZINC 03861600		H	OH	OH	H
8	NSC 119910		H	OH	OH	H	21	NSC 119893		H	OH	OH	H
9	ZINC 03860685		OH	H	H	OH	22	ZINC 04822213		OH	H	H	OH
10	ZINC 13597410		OH	H	H	OH	23	ZINC 04582279		H	H	H	H
11	ZINC 05030632		H	H	H	H	24	NSC 119912		H	OH	OH	H
12	NSC 119888		H	H	H	H	25	NSC 119916		H	OH	OH	H
13	ZINC 05030658		H	H	H	H							

3.2 Effect of the close analogs of NSC 119915 on the phosphatase activity of purified recombinant forms of CDC25

As a primary approach to the identification of novel structures with increased inhibition potency towards CDC25, we have evaluated the inhibition properties of the close analogs of **NSC 119915** through a fluorimetric assay, that measured the residual phosphatase activity of the

recombinant form of CDC25B in the presence of the various compounds. Among the twenty-five molecules selected from the multiple ligand-based chemoinformatic approach, eight compounds (**2**, **10**, **12-14**, and **16-18**) were excluded from the analysis, because endowed with a strong fluorescent signal, which interfered with the emission wavelength of the synthetic substrate OMFP used in the fluorimetric assay. The inhibition of the phosphatase activity of CDC25B by the remaining seventeen analogs was evaluated in the presence of two different concentrations of these compounds (Table 2).

Table2: Residual phosphatase activity of CDC25B in the presence of compound NSC 119915 or its 6-xanthone analogs

Results

Cpd	CDC25B residual activity (%) in the presence of [inhibitor]	
	0.2 μM	1 μM
1	76	9
3	85	62
4	90	28
5	12	2
6	14	2
7	44	1
8	10	1
9	9	0
11	89	44
15	79	18
19	86	70
20	91	24
21	13	1
22	80	0
23	80	14
24	22	3
25	24	1
NSC 119915	38	2

The data indicated that nine compounds (**1**, **3**, **4**, **11**, **15**, **19**, **20**, **22**, and **23**) caused a measurable inhibition of the phosphatase activity, only when added at the highest concentration. Therefore, most of these compounds were excluded from the following analysis. In contrast, eight analogs (**5-9**, **21**, **24**, and **25**), all of them containing a 6-xanthone chemical motif, exerted a concentration-dependent inhibition of the CDC25B phosphatase activity, with a percentage of inhibition comparable to that exhibited by the lead compound **NSC 119915**. Therefore, these eight analogs were

chosen for the following studies and one compound from the less active group, *i.e.* cpd **3**, was included in the subsequent analysis.

To better investigate the inhibition properties of the effective analogs, their K_i values were determined, using the three different CDC25 proteins. Figure 4 shows the kinetic evaluation of the inhibitory effect exerted by one of these compounds, *i.e.* cpd **7**, on the three CDC25 forms. Indeed, the behaviour of this compound was similar to that observed with the other 6-xanthone derivatives; therefore, the behaviour of **7** was considered as representative of the inhibition mechanism exerted by all these compounds.

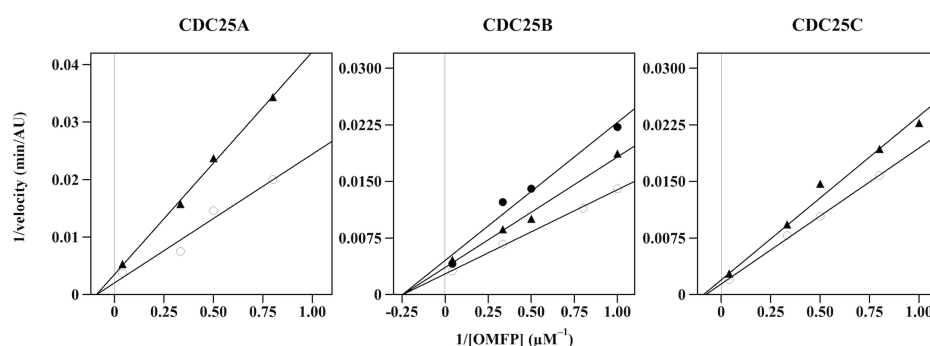


Figure 4: Effect of compound 7 on the Lineweaver-Burk plots of the A. CDC25A B. CDC25B and C. CDC25C phosphatase activity. The phosphatase activity was measured through the rate of OMFP hydrolysis as described in the Materials and Methods. The activity was determined either in the absence (empty circles in **A.**, **B.** and **C.**) or in the presence of the following concentrations of compound 7: 0.5 μM (filled triangles in **A.**), 0.25 μM or 0.5 μM (filled triangles or filled circles, respectively, in **B.**), 1 μM (filled triangles in **C.**).

The K_i of the tested compounds towards the three different CDC25 forms are reported in Table 3; their low values confirmed that these compounds possessed a strong inhibition towards CDC25A, -B or -C. Indeed, the measured K_i values obtained for the 6-xanthone derivatives were similar to that determined for NSC 119915 and all comprised in relatively small intervals; in particular, the K_i towards CDC25A ranged between 0.01 and

0.80 μM , and the corresponding intervals for CDC25B and CDC25C were 0.12 – 2.4 μM and 0.30 – 4.4 μM , respectively. Among the three forms, CDC25A showed a slightly higher sensitivity towards the inhibitors, whereas CDC25C had a moderately lower responsiveness. Concerning the mechanism of inhibition exerted by the 6-xanthone analogs, the kinetic measurements showed that the tested compounds had a behavior similar to that already reported for NSC 119915 [24]. In particular, in the presence of the inhibitors, the K_M value for the substrate OMFP was not essentially modified, whereas the V_{\max} of phosphatase activity was significantly reduced. Therefore, the tested analogs of NSC 119915 were non-competitive inhibitors of CDC25 and probably acted in an irreversible manner.

Table 3: K_i values of compound NSC 119915 or its 6-xanthone analogs towards CDC25A, -B, -C phosphatases

Cpd	K_i (μM)		
	CDC25A	CDC25B	CDC25C
3	0.28 \pm 0.09	2.4 \pm 0.39	4.4 \pm 0.62
5	0.38 \pm 0.12	0.12 \pm 0.05	0.39 \pm 0.15
6	0.10 \pm 0.03	1.1 \pm 0.37	1.0 \pm 0.41
7	0.65 \pm 0.04	0.78 \pm 0.03	3.1 \pm 0.22
8	0.17 \pm 0.07	0.19 \pm 0.08	0.30 \pm 0.12
9	0.80 \pm 0.31	0.44 \pm 0.2	1.5 \pm 0.48
21	0.14 \pm 0.06	0.14 \pm 0.05	0.63 \pm 0.14
24	0.01 \pm 0.005	0.3 \pm 0.08	0.40 \pm 0.11
25	0.40 \pm 0.15	1.1 \pm 0.4	0.96 \pm 0.38
NSC 119915	0.34 \pm 0.12	0.10 \pm 0.04	0.24 \pm 0.13

3.3 Evaluation of CDC25 inhibitors on cell growth rate of A2058 and SAN melanoma cells

The potent antiproliferative action of NSC 119915 on some cancer cell lines deriving from breast or prostate carcinoma, as well as from acute myeloid leukemia, was recently described [24]. In the present work the biological effects of these compounds were evaluated, using two melanoma cell lines, *i.e.* A2058 and SAN, as a cellular system. The cytotoxic effects of the lead compound and its analogs on the growth rate of the melanoma cell lines was investigated. In particular, the effect of the inhibitors was monitored after different times of treatment with 25, 50 or 100 μ M NSC 119915 or its analogs **3**, **5-9**, **21**, and **24-25**. Figure 5 shows the cell growth rate of A2058 and SAN cells after 48-h treatment in the presence of 100 μ M of the various compounds. This concentration was considered the minimum dose of inhibitor that caused an evident cytotoxic activity in melanoma cells. As shown in Figure 5A, only the

analog **7**, among the nine compounds, caused a significant reduction of the cell growth rate of A2058, whereas the other 6-xanthone derivatives, as well as **NSC 119915**, were quite ineffective or caused a not significant reduction of cell growth rate. A similar behavior was observed after 72-h incubation, because only cpd **7** provoked the significant reduction of cell growth rate (data not shown). Figure 5B reports the effects of the inhibitors in SAN cells. Three compounds, i.e. **6**, **7** and **24**, caused a significant reduction of cell growth rate after 48-h treatment; however, when the treatment was prolonged up to 72 h, also compound **NSC 119915** exerted a significant reduction of cell growth rate (not shown). Therefore, cpd **7**, showing its cytotoxicity in both cell lines starting from 48-h treatment, was considered as representative of the effect of this group of molecules in melanoma cells and was used for further experiments.

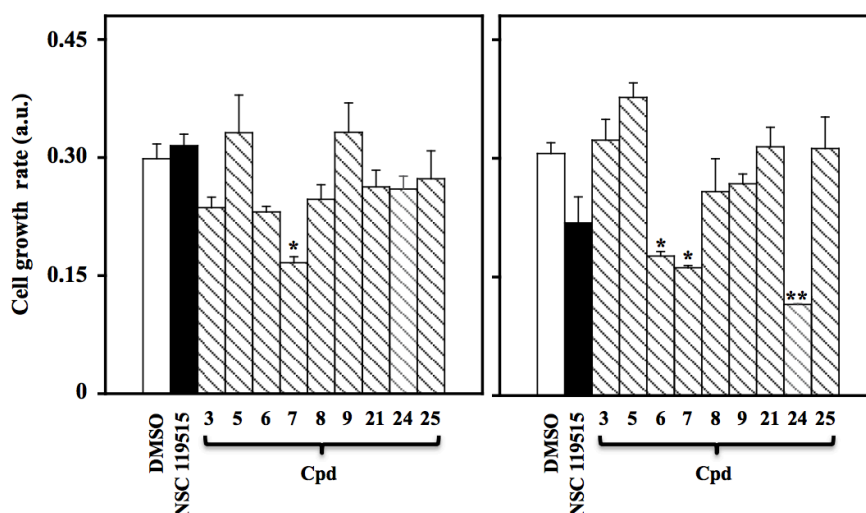


Figure 5: Effect of NSC 119915 and its close analogs on cell growth rate of melanoma cells. A. A2058 and B. SAN cells were incubated for 48 h with 0.5% DMSO as a vehicle control or 100 μ M of each of the indicated compounds. The cell growth rate is reported as arbitrary units (a.u.). Data from four independent experiments are reported as the means \pm SE. * p < 0.05 and ** p < 0.01 compared to control cells.

3.4 Effect of compound 7 on cell cycle progression and apoptosis

CDC25 phosphatases are crucial regulators of cell cycle and for this reason, the effect of **7** on cell cycle progression was studied in detail. To this aim, asynchronously growing A2058 cells were treated at different times with 100 μ M cpd **7**, and then cell cycle analysis was cytofluorimetrically monitored after PI incorporation. Figure 6 shows the time-dependent distribution of the cell cycle in its different phases. In particular, after 16-h incubation with vehicle alone, cells were mainly and almost equally distributed in G0/G1 and G2/M phases (the ratio between them being 0.96), with an almost undetectable representation in the S-phase; conversely, after 16-h treatment with cpd **7**, a significant decrease of cells in G0/G1 phase was evident, accompanied by a remarkable improvement of the G2/M cell arrest (the ratio between G0/G1 and G2/M decreased to 0.38), as shown in Figure 6A. If the incubation with the cpd **7** was prolonged up to 24 h, the distribution of the different phases of cell cycle was essentially identical to that obtained at 16 h (Figure 6B).

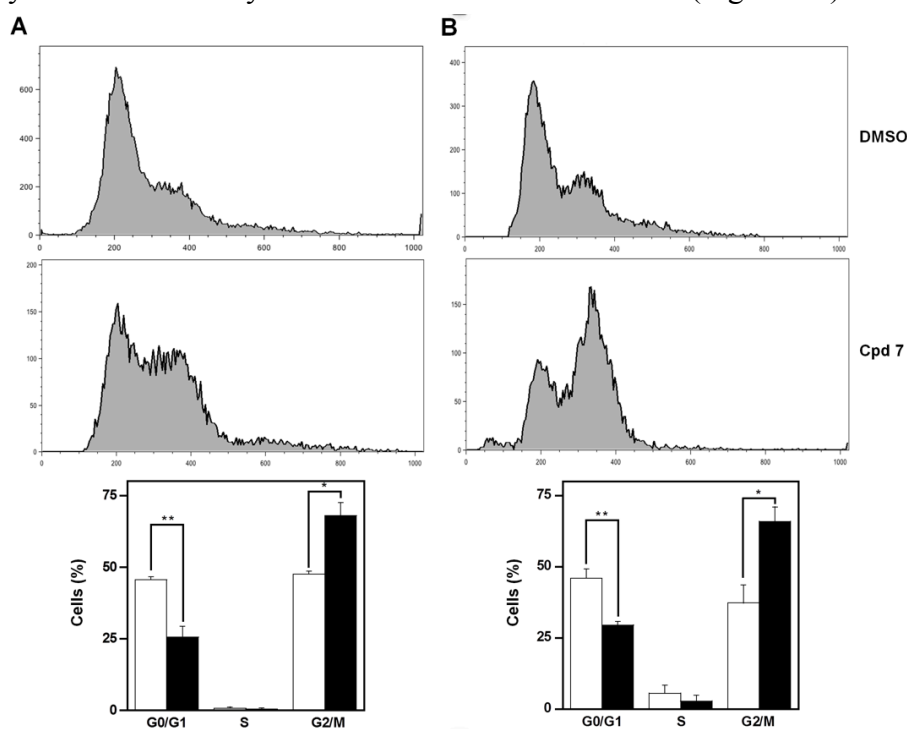


Figure 6: Effect of compound 7 on the distribution of cell cycle phases of A2058 cells. The determination of cells in the different phases was evaluated after **A.** 16 h or **B.** 24 h from treatment with 0.5% DMSO or 100 μ M compound 7, as described in the Materials and Methods. Histograms, which show the cell percentage among the various phases, were obtained from triplicate experiments and reported as the means \pm SE. * p < 0.05 and ** p < 0.01 compared to control cells. Vehicle alone, open bars; compound 7, black bars.

Furthermore, a similar general picture emerged from the effect of cpd 7 on cell cycle progression of SAN cells (Figure 7).

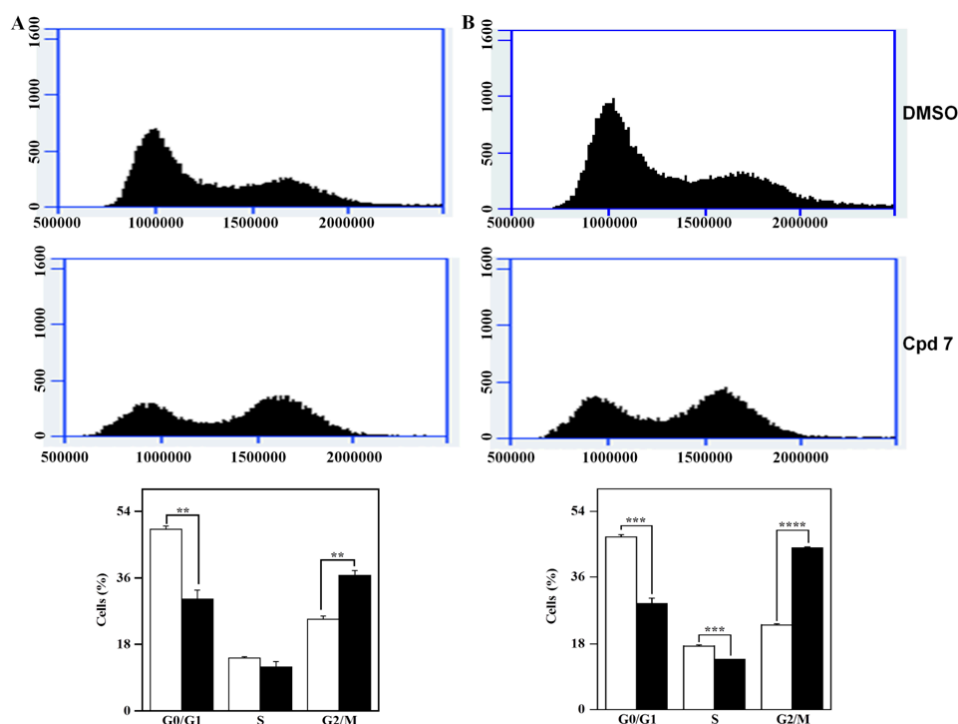
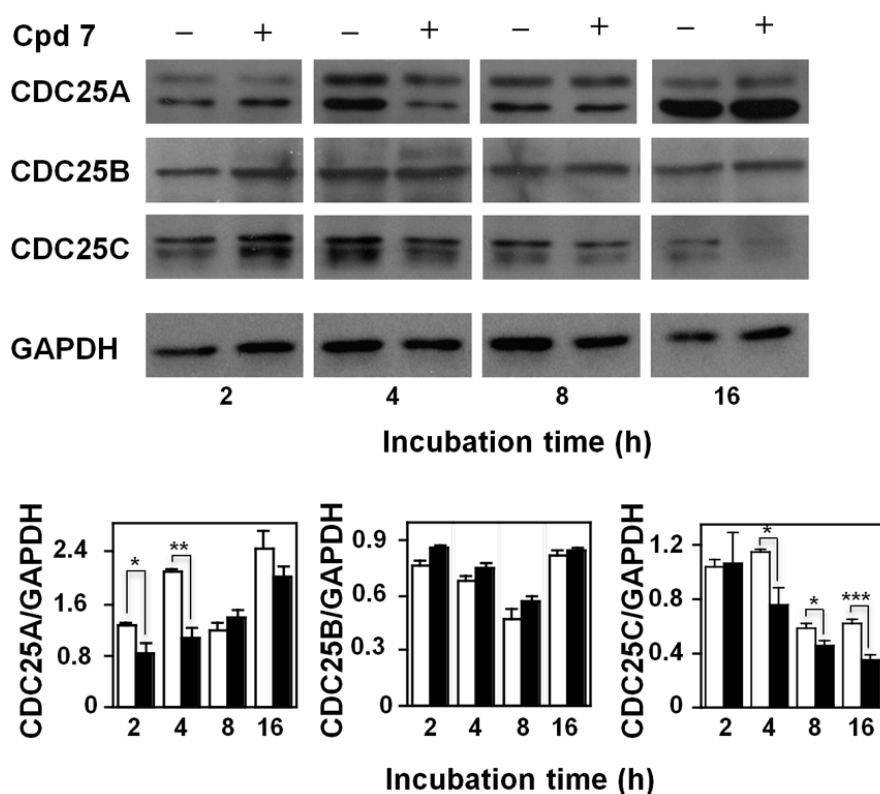


Figure 7: Effect of compound 7 on the distribution of cell cycle phases of SAN cells. The determination of cells in the different phases was evaluated after (A) 16 h or (B) 24 h from treatment with 0.5 % DMSO or 100 μ M compound 7, as described in the Materials and Methods. Histograms, which show the cell percentage among the various phases, were obtained from triplicate experiments and reported as the means \pm SE. ** p < 0.01, *** p < 0.001 and **** p < 0.001 compared to control cells. Vehicle alone, open bars; compound 7, black bars.

Considering that CDC25 phosphatases are key cell cycle regulators, and that the previous *in vitro* data indicated that cpd 7 was a potent inhibitor of this important enzyme, we have investigated the cytotoxic effect of this compound at the molecular level. In particular, we have evaluated if the treatment of A2058 cells with 7 affected also the protein levels of the three CDC25 forms. The Western blotting analysis reported in Figure 8 shows that compound 7 induced a reduction of both CDC25A and CDC25C protein levels. In particular, an early decrease of the CDC25A was observed up to 4 h compared to untreated cells. A progressive and significant reduction of the CDC25C protein levels was observed starting from 4 h and continuing at least up to 16 h. On the other hand, the protein levels of CDC25B were not affected by treatment of A2058 cells with 7.



Results

Figure 8: Effect of compound 7 on CDC25A, B and C protein levels. Total protein extracts from A2058 cells, incubated with 0.5% DMSO (open bars) or 100 μ M compound 7 (black bars) for 2, 4, 8 or 16 h, were analyzed by Western blotting. GAPDH was used as loading control. The doublets observed in the immunoblots detecting CDC25A or CDC25C were due to the common presence of multiple isoforms of these proteins. Densitometric analysis is shown in the lower panel. Data from triplicate experiments were reported as the means \pm SE. * p < 0.05, ** p < 0.01, *** p < 0.001, compared to control cells. Other details as described in the Materials and Methods.

An earlier reduction of CDC25C protein levels was observed even in SAN cells treated with cpd 7 (Figure 9). Therefore, the arrest of both melanoma cells in G2/M phase could be also related to a modulation of the CDC25 protein levels induced by 7.

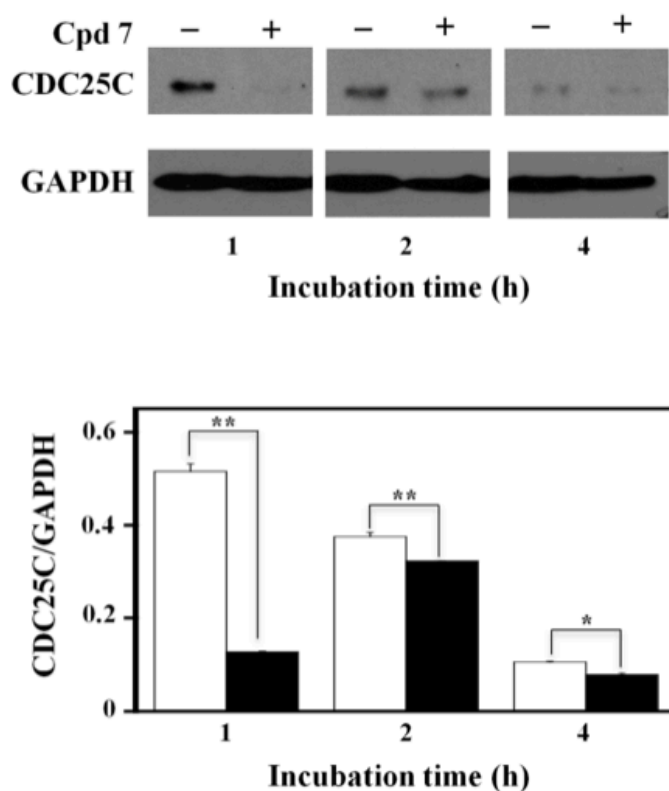


Figure 9: Effect of compound 7 on CDC25C protein levels. Total protein extracts from SAN cells, incubated with 0.5 % DMSO (open bars) or 100 μ M compound 7 (black bars) for 1, 2, or 4 h, were analyzed by Western blotting. GAPDH was used as loading control. Densitometric analysis is shown in the lower panel. Data from triplicate experiments were reported as the means \pm SE. * $p < 0.05$, ** $p < 0.01$, compared to control cells. Other details as described in the Materials and Methods.

The effect of 7 on cell growth and cycle progression could suggest the beginning of a cell death program. This hypothesis was investigated through various methodological approaches. It is known that the number of nuclei with a sub-diploid content is a typical hallmark of apoptosis. To this aim, PI incorporation was carried out by a flow cytometric analysis after treatment of melanoma cells with 100 μ M cpd 7. A time-dependent increase of apoptosis was evident in A2058 cells (Figure 10A). In particular, the effect of 7 on the cell death program became significant already at 48 h, and after 72-h incubation, a 18-fold increase of apoptosis was reached. Interestingly, after 72-h incubation of SAN cells, a similar 16-fold increase of apoptotic cells was observed upon treatment with 100 μ M cpd 7 (Figure 10B). Furthermore, to better investigate the capacity of 7 to induce apoptosis, the enzymatic activity of caspase-3, the final effector of the apoptotic program, was monitored. Hence, caspase-3 activity was spectrofluorimetrically measured in both melanoma cells after a 24-h treatment with 100 μ M cpd 7. As clearly shown for A2058 (Figure 10C) and SAN cells (Figure 10D), this inhibitor provoked a significant increase of the enzymatic activity of caspase-3.

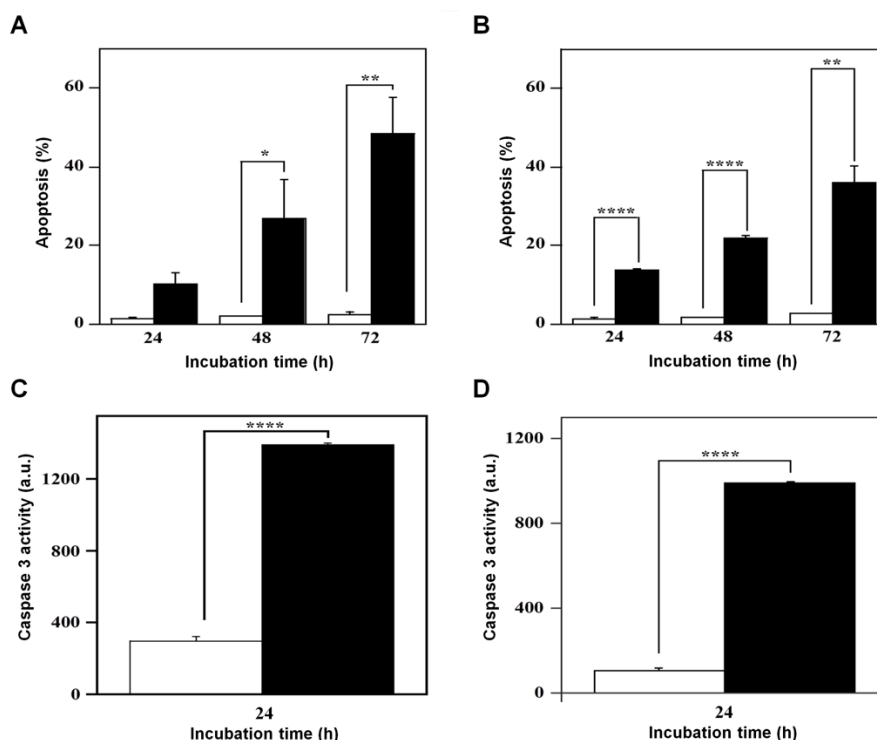


Figure 10: Effect of compound 7 on the apoptosis of A2058 and SAN cells. The apoptotic process was evaluated in A2058 (panels A. and C.) and SAN (panels B. and D.) cells either through the determination of the number of cells with a subdiploid DNA content (A. and B.) or by measuring the caspase-3 enzymatic activity (C. and D.). Cells were treated with 0.5% DMSO (open bars) or 100 μ M compound 7 (black bars) for the indicated incubation times. Apoptosis was expressed as a percentage, whereas caspase-3 activity was reported as arbitrary units (a.u.). Data from triplicate experiments were reported as the means \pm SE. * p < 0.05, ** p < 0.01, **** p < 0.0001, compared to control cells. Other details as described in the Materials and Methods.

To confirm that the pro-apoptotic effect of 7 was caspase-mediated, the 48-h treatment of A2058 and SAN cells with cpd 7 was also carried out in the presence of an irreversible pan-caspase inhibitor, such as Z-VAD-FMK. The data reported in Figure 11 indicate that the level of apoptosis caused by 7 was significantly decreased in the presence of the pan-caspase inhibitor in either A2058 or SAN cells, thus demonstrating that the pro-apoptotic effect of 7 was mainly caspase-dependent. These overall

data support the hypothesis that cell cycle arrest in G2/M phase caused by **7** could evolve in an apoptotic process.

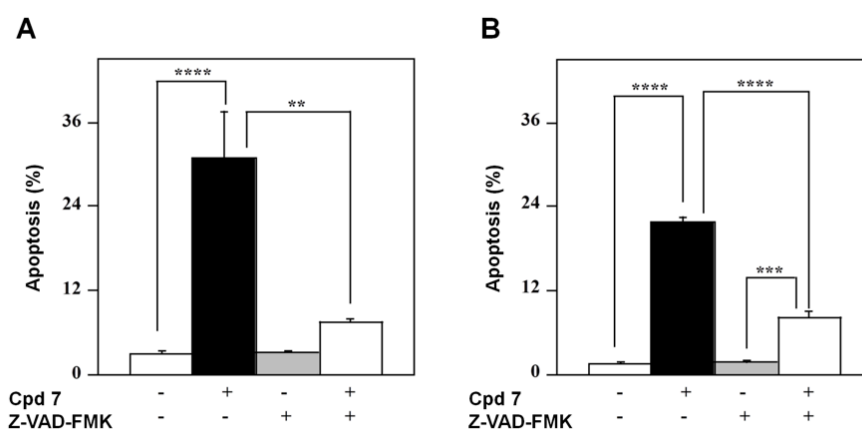


Figure 11: Effect of Z-VAD-FMK, a pan-caspase inhibitor, on the apoptotic process induced in melanoma cells by compound **7.** A2058 (panel A.) and SAN (panel B.) cells were treated with 0.5% DMSO or 100 μ M compound **7** and incubated in the absence or in the presence of 100 μ M Z-VAD-FMK; the apoptosis was evaluated after a 48-h incubation through the determination of the number of cells with a subdiploid DNA content. Data from triplicate experiments were reported as the means \pm SE. ** $p < 0.01$, *** $p < 0.001$ and **** $p < 0.0001$ compared to respective control cells. Other details as described in Materials and Methods.

3.5 Effect of compound **7** on ROS generation and mitochondrial membrane potential

It is known that the high redox reactivity of quinonoid molecules, like cpd **7**, could greatly perturbate the intracellular redox state. To this aim, the intracellular ROS level was monitored in melanoma cells after their treatment with 100 μ M cpd **7**. Indeed, a time-dependent increase of the ROS level was observed upon treatment of A2058 cells with the inhibitor **7**, that became significant already after 4-h (Figure 12A). Furthermore, we have also evaluated the possible reversion of the oxidant effect of **7** in the presence of a broad-range antioxidant molecule, such as NAC, or the

specific inhibitor of NADPH oxidase apocynin. To this aim, A2058 cells were pre-incubated for 1 h with 10 mM NAC or for 45 min with 0.5 mM apocynin, and then treated for 4 h with the inhibitor **7**. As clearly shown in Figure 12B, only NAC prevented the increase of ROS level, whereas apocynin was unable to revert this increase. We have also evaluated if the increase of ROS level caused by cpd **7** could mediate the observed apoptotic process induced by this inhibitor. Indeed, the increase of the number of apoptotic cells observed upon 48-h treatment with 100 μ M compound **7** was in a great part reverted by the cellular pre-treatment with NAC (Figure 12C).

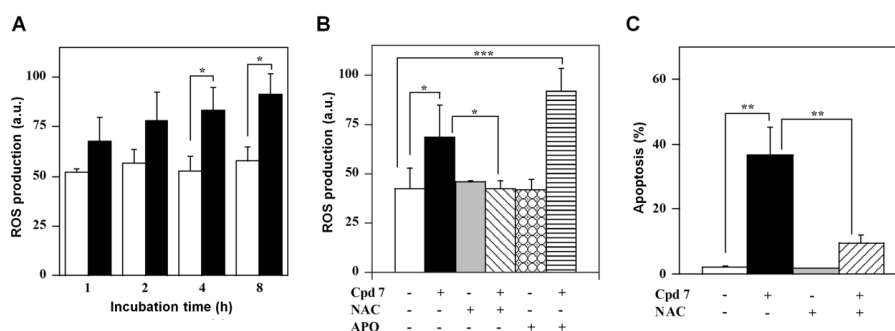


Figure 12: ROS production and their involvement in the apoptotic process of A2058 cells, as induced by treatment with compound **7.** **A.** Time-dependent measurement of ROS production. Cells were incubated with 0.5% DMSO (open bars) or 100 μ M compound **7** (black bars) and then the intracellular ROS level was measured. **B.** Effect of antioxidant molecules on ROS production. The ROS level was also measured in cells untreated or pretreated with NAC or apocynin after a 4-h incubation with DMSO or **7**. **C.** Effect of NAC on apoptosis. The PI incorporation was evaluated in cells untreated or pretreated with NAC after a 48-h incubation with DMSO or **7**. ROS production was expressed as a.u., and apoptosis as a percentage. Data from triplicate experiments were reported as the means \pm SE. * p < 0.05 and ** p < 0.01 compared to control cells. Other details as described in the Materials and Methods.

As clearly shown in Figure 13, the same overall picture was observed also with SAN cells. Therefore, all these results suggest that **7** altered the intracellular redox state of melanoma cells, thus mediating the observed

cytotoxicity.

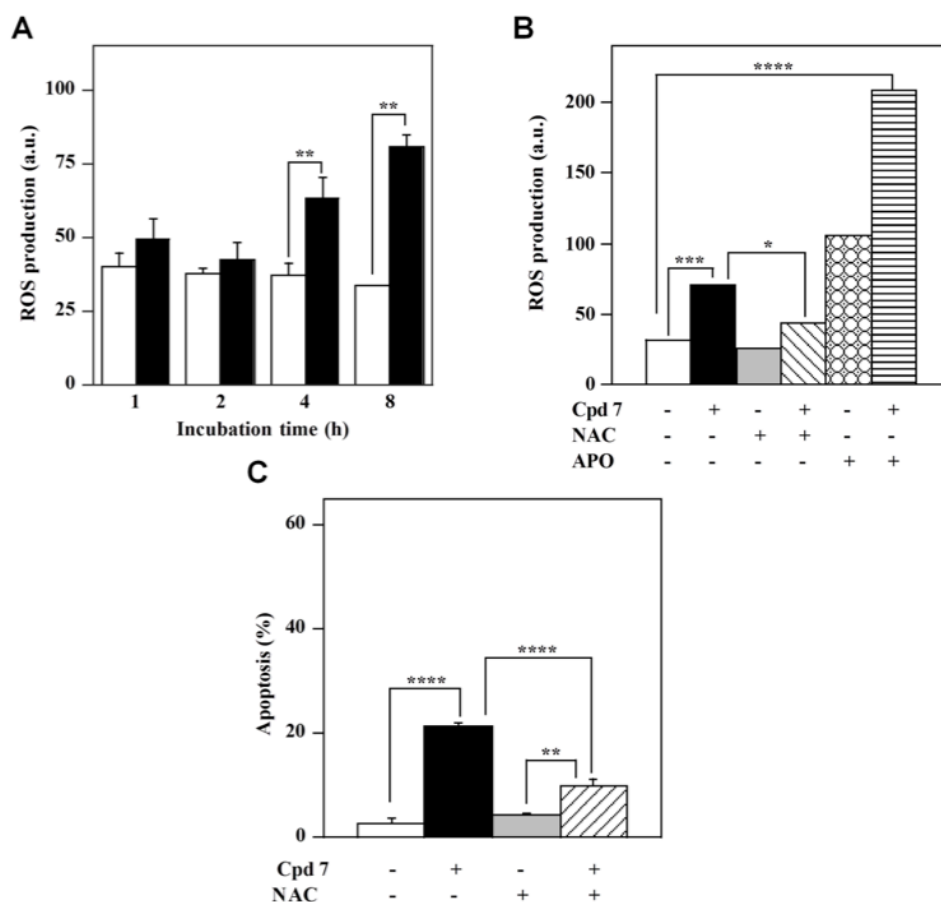


Figure 13: ROS production and their involvement in the apoptotic process of SAN cells, as induced by treatment with compound 7. (A) Time-dependent measurement of ROS production. Cells were incubated with 0.5 % DMSO (open bars) or 100 μ M compound 7 (black bars) and then the intracellular ROS level was measured. (B) Effect of antioxidant molecules on ROS production. The ROS level was also measured in cells untreated or pretreated with NAC or apocynin after a 4-h incubation with DMSO or 7. (C) Effect of NAC on apoptosis. The PI incorporation was evaluated in cells untreated or pretreated with NAC after a 48-h incubation with DMSO or 7. ROS production was expressed as a.u., and apoptosis as a percentage. Data from triplicate experiments were reported as the means \pm SE. * $p < 0.05$, ** $p < 0.01$, *** $p < 0.001$ and **** $p < 0.0001$ compared to relative control cells. Other details as described in the Materials and Methods.

Mitochondria represent the primary source of ROS, as well the target of ROS action; therefore, we have investigated if the treatment of melanoma cells with cpd **7** could affect the mitochondrial functionality. To this aim, the variation of the mitochondrial membrane potential was fluorimetrically monitored after a time-dependent incubation of A2058 cells with **7**. This molecule provoked a reduction of the fluorescent signal, corresponding to a decrease of the mitochondrial membrane potential, that was already evident after 24 h and then continued at least up to 72 h (Figure 14A). Proteins belonging to the B-cell lymphoma-2 (Bcl-2) family are involved in the modulation of the mitochondrial functionality [32,33]. Hence, we have assessed the levels of the anti-apoptotic protein Bcl-2, as well as that of the pro-apoptotic Bcl-2-associated X protein (Bax), in A2058 cells after incubation with **7** (Figure 14B). As clearly shown in the densitometric analysis (Figure 14C), the incubation with the inhibitor caused a clear reduction of the bcl-2 level after 8-h treatment, and this decrease was still evident after 16 h; on the other hand, a clear increase of Bax was observed after 16-h incubation with **7**. The densitometric analysis also shows the value of the Bcl-2/Bax ratio, because its significant reduction observed after 8 and 16 h represents a better tool to reveal the regulation of the apoptotic process by **7** (Figure 14C). Therefore, the increase of ROS, the reduction of mitochondrial membrane potential, and the modulation of the protein levels of members of the Bcl-2 family suggest the occurrence of a mitochondrial-mediated apoptosis induced by compound **7**. This hypothesis was further supported by the increase of caspase-9 activity measured in A2058 cells after 24-h incubation with **7** (Figure 14D).

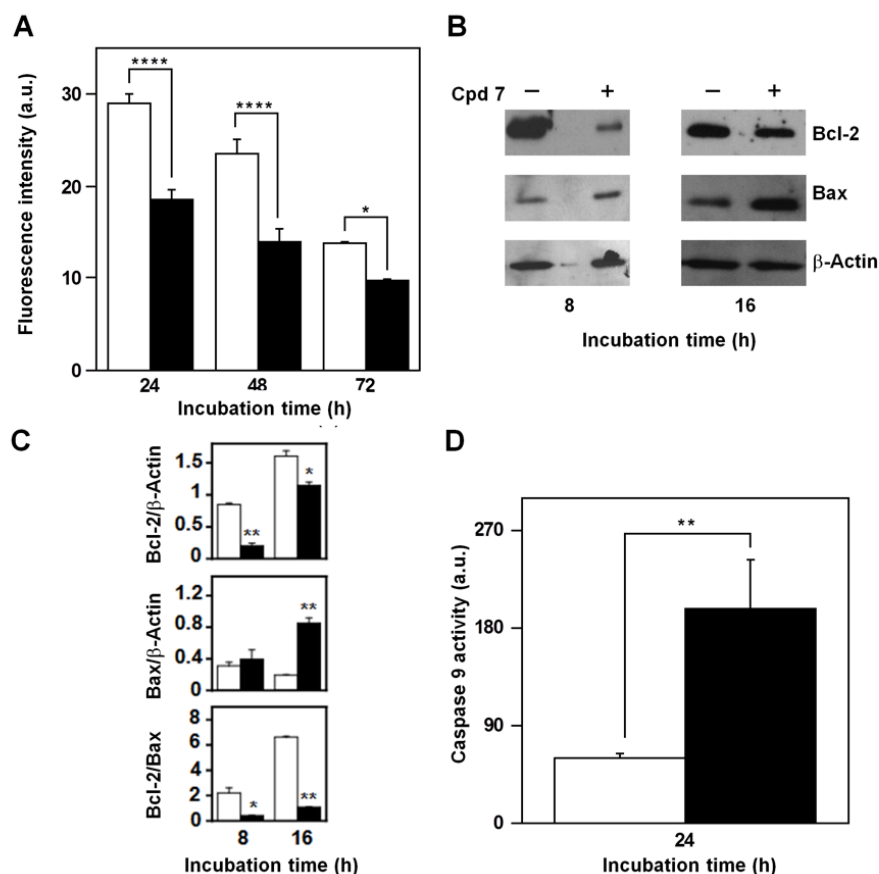


Figure 14: Effect of compound 7 on some apoptotic mitochondrial markers in A2058 cells. **A.** Measurement of the mitochondrial membrane depolarization. Cells were treated for the indicated times with 0.5% DMSO (open bars) or 100 μM compound 7 (black bars). **B.** Evaluation of Bcl-2 and Bax protein levels. Total protein extracts from A2058 cells, incubated with 0.5% DMSO or 100 μM compound 7 for 8 or 16 h, were analyzed by Western blotting. β-actin was used as loading control. **C.** Densitometric analysis of the Bcl-2 and Bax protein levels, as well as of the Bcl-2/Bax ratio. **D.** Determination of the caspase-9 enzymatic activity. Total protein extracts from A2058 cells, incubated with 0.5% DMSO (open bars) or 100 μM compound 7 (black bars) for 24 h, were assayed for caspase-9 activity. Data from triplicate experiments were reported as the means ± SE. * $p < 0.05$, ** $p < 0.01$, **** $p < 0.0001$, compared to control cells. Other details as described in the Materials and Methods.

The effect of compound 7 was evaluated also in SAN cells and almost

overlapping results were obtained (Figure 15). All these findings suggest that the increase of ROS levels associated to an alteration of typical mitochondrial markers could contribute or mediate the cytotoxic effect exerted by **7** in melanoma cells.

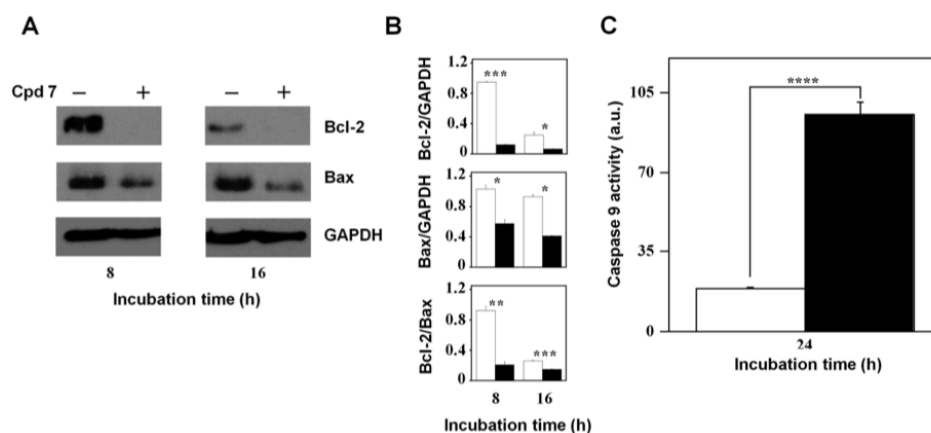


Figure 15: Effect of compound 7 on some apoptotic mitochondrial markers in SAN cells. (A) Evaluation of Bcl-2 and Bax protein levels. Total protein extracts from SAN cells, incubated with 0.5 % DMSO or 100 μ M compound **7** for 8 or 16 h, were analyzed by Western blotting. GAPDH was used as loading control. (B) Densitometric analysis of the Bcl-2 and Bax protein levels, as well as of the Bcl-2/Bax ratio. (C) Determination of the caspase-9 enzymatic activity. Total protein extracts from SAN cells, incubated with 0.5 % DMSO (open bars) or 100 μ M compound **7** (black bars) for 24 h, were assayed for caspase-9 activity. Data from triplicate experiments were reported as the means \pm SE. * $p < 0.05$, ** $p < 0.01$, **** $p < 0.0001$, compared to control cells. Other details as described in the Materials and Methods.

3.6 Effect of compound 7 on Akt activation and p53 protein levels

It is known that one of the key proteins involved in the control and regulation of cell survival is the kinase B, Akt, in its phosphorylated form (pAkt) [34,35]. The molecular mechanisms that regulate the cytotoxic potential of cpd **7** were further investigated through the evaluation of the activation state of Akt. Therefore, the protein levels of pAkt have been analysed after 2- and 4-h incubation of A2058 cells with **7**. As shown in Figure 16A, the inhibitor caused an early decrease of the pAkt protein

level with respect to total Akt; indeed, this reduction was already evident after 2-h and remained detectable until 4-h incubation. An early decrease of Akt activation was observed also in SAN cells (not shown).

It is known that Akt regulates the process of cell survival by phosphorylating different substrates, directly or indirectly involved in the apoptotic program [36]. One of these targets is p53, a protein with a tumor-suppressor activity that regulates the cell cycle, as well as the expression of several genes involved in the apoptosis. In detail, Akt negatively regulates the apoptosis, by enhancing the degradation of p53 via its phosphorylation, as well as by promoting the nuclear localization and binding of this factor to human murine double-minute 2 (MDM2) protein, a negative regulator of p53 [36]. Hence, we tested if the treatment of melanoma cells with the CDC25 inhibitor **7** could affect the protein levels of p53. As shown in Figure 16B, the increase of p53 level, already evident after 8-h incubation, became significant after 16-h incubation. Also in SAN cells a time-dependent decrease of the basal level of p53 was observed (not shown). Therefore, it could be envisaged that the early reduction of pAkt represents an upstream event that triggers other molecular events, such as the increase of p53, thus contributing to the cytotoxic effect exerted by **7** in melanoma cells.

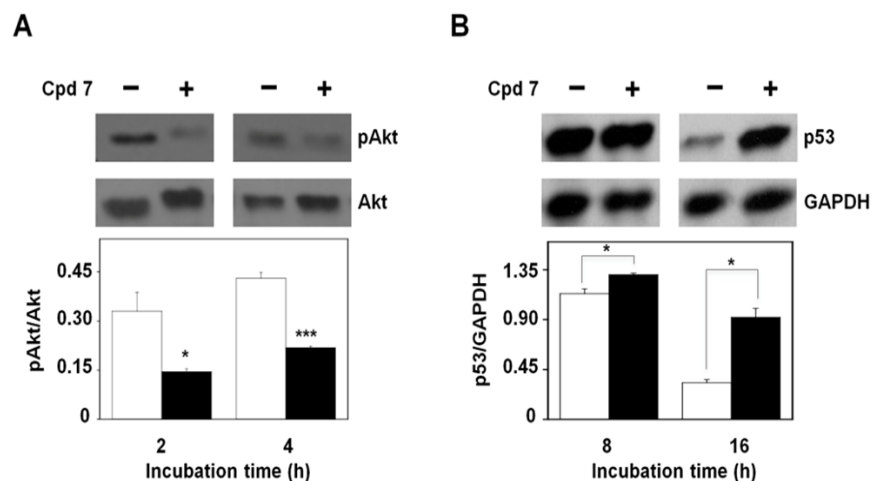


Figure 16: Effect of compound 7 on pAkt and p53 protein levels. **A.** Evaluation of pAkt protein levels. Total protein extracts from A2058 cells, incubated with 0.5% DMSO or 100 μ M compound 7 for 2 or 4 h, were analyzed by Western blotting using an antibody raised against pAkt (Ser473). Akt was used as loading control. Densitometric analysis shown in the lower panel. **B.** Evaluation of p53 protein levels. Total protein extracts from A2058 cells, incubated with 0.5% DMSO or 100 μ M compound 7 for 8 or 16 h, were analyzed by Western blotting. GAPDH was used as loading control. Densitometric analysis shown in the lower panel. Data from triplicate experiments were reported as the means \pm SE. * $p < 0.05$, *** $p < 0.001$, compared to control cells. Other details as described in the Materials and Methods.

4. DISCUSSION AND CONCLUSIONS

The aim of this thesis was the discovery of new inhibitors of CDC25 phosphatases, because of the potential oncogenic nature of these enzymes [8,13]. In particular, the usage of these new molecules in a possible therapeutic strategy against melanoma was considered, because it is known that this tumor is highly metastatic and very refractory to any conventional therapy [37,38]. A previous investigation from this laboratory led to the characterization of a novel and potent inhibitor of CDC25, **NSC 119915**, possessing a quinonoid structure [24]. This compound acted as an irreversible inhibitor of CDC25 and was endowed with a cytotoxic activity towards various cancer cell lines. In order to ameliorate the inhibitory power of this compound, different chemoinformatic approaches were combined [39,40] and led to the design of 126 potential inhibitors of CDC25 proteins. Among them, 25 top-ranked close analogs of our lead compound **NSC 119915** were chosen and synthesized, because they were expected to possess inhibitory activity against the CDC25A, -B and -C phosphatases. Interestingly, among the 25 candidates, eight compounds, sharing the same 6-xanthone motif (**5-9**, **21**, **24**, and **25**), caused an *in vitro* dose-dependent inhibition of the CDC25B phosphatase activity. Kinetic analyses revealed that these compounds inhibited the three different CDC25 proteins in a noncompetitive manner with K_i values comparable to those of the lead compound **NSC 119915**. Only slight differences were found in the inhibition power towards the three CDC25 forms, CDC25A being slightly higher sensitive towards the inhibitors, and CDC25C having a moderately lower responsiveness.

When melanoma is diagnosed at a late stage, it becomes one of the more aggressive tumours, frequently linked to a poor prognosis. As CDC25 phosphatases, in combination with other cell cycle regulators, are involved in melanoma growth and progression [25,41], we have decided to evaluate the effects of **NSC 119915** and its close analogs, *i.e.* the eight potent inhibitors **5-9**, **21**, **24**, and **25** and the weak inhibitor **3**, on the growth rate of two melanoma cell lines, A2058 and SAN. The results of this investigation showed that only one analog, cpd **7**, was capable to reduce the cell growth rate of both A2058 and SAN melanoma cells.

However, in SAN cells, also the analogs **6** and **24**, as well as in some experimental conditions also NSC **119915**, caused a significant decrease of the cell growth rate. The failure of compounds **5**, **8**, **9**, **21** and **25** to inhibit cell proliferation, despite their *in vitro* potent inhibition of all three CDC25 phosphatases, could be due to poor permeability into cells, chemical instability, unfavourable compartmentalization, active metabolism into inactive compounds, presence of unidentified binding proteins, or a combination of these factors. In conclusion, for its common behavior in both melanoma cell lines, **7** was selected as the most promising compound for further investigation of its antimelanoma effects. CDC25s are fine regulators of the different phases of cell cycle. Hence, we checked if the reduction of cell growth rate caused by **7** was associated to an alteration of cell cycle progression. A significant reduction of the G0/G1 phase and an increase of the G2/M phase occurred in both melanoma cells lines after 16-h treatment and continued up to 24-h. It is known that many cytotoxic compounds, as well as various anti-cancer drugs, cause DNA damage [42,43]. This event activates different checkpoint pathways, which can induce an arrest of cell proliferation, thus enabling cells to DNA repair in order to prevent cell death. On the other hand, if the mechanisms involved in the DNA repair are ineffective and the DNA damage is not completely repaired, cells can be committed to programmed cell death. As CDC25 proteins exert a pivotal role in the regulation of cell division cycle [8], their overexpression might facilitate checkpoint exit and contribute to neoplastic transformation. Hence, CDC25 inhibition, inactivation or degradation can amplify the cytotoxic activity of some compounds. The treatment of melanoma cells with cpd **7** caused a modulation of the CDC25 protein levels. In particular, we observed an early reduction of CDC25A associated to a progressive and strong decrease of CDC25C. These results suggest that the observed G2/M arrest of cell cycle in melanoma cells could depend on an inhibition of phosphatase activity of CDC25 proteins, as well as on a reduction of the protein levels of CDC25A and, more consistently, of CDC25C. This behavior seems in good agreement with the major role played by CDC25C in the control of the G2/M progression of cell cycle [44]. The reduction of cell growth rate and the G2/M block of cell cycle could

evoke the beginning of a cell death program. Indeed, cpd **7** activated a time-dependent apoptotic program in melanoma cells, as revealed by PI incorporation experiments and measurements of caspase-3 activity. Hence, we can infer that the apoptosis observed in melanoma cells represents a consecutive process to the long cell cycle blockage in the G2/M phase.

It is known that quinonoid structures, as those of the most active CDC25 inhibitors, are good substrates for the beginning of a redox cycle, and that an increased ROS level may cause severe damages to the CDC25 structure [20,45,46]. Indeed, quinonoid compounds exert their inhibitory activity on CDC25 through the oxidation of cysteine residues located in the active site [21,24]. On the other hand, the increase of ROS level may be deleterious also to other cellular components, thus activating various metabolic pathways that control the cell cycle. Compound **7** induced an increase of the intracellular ROS levels in both melanoma cells, an event reverted by NAC, whereas apocynin was ineffective. It is known that NAC is the precursor of glutathione, the main intracellular antioxidant, and that the target of apocynin is NADPH oxidase, the most important ROS source located on the membrane. The different effect exerted by these two antioxidant molecules led to the speculation that lipophilicity of **7** could allow its efficient crossing through the cellular membrane; however, the presence of some polar groups in **7** probably prevents its stable interaction with the inter-membrane components, such as NADPH oxidase. However, the reversion of apoptosis in the presence of NAC suggests that the increase of intracellular ROS levels may be considered as an early event involved in the signalling triggered by cpd **7**.

The apoptotic machinery is an essential element of cell cycle checkpoints and the cytotoxic effects of many drugs are mediated by mitochondrion through the activation of an intrinsic apoptotic pathway. Bcl-2 family members play a role not only in the regulation of apoptosis but also in the control of cell cycle [47]. In this work, the observed increase of ROS levels, as well as the decrease of the crucial parameter for controlling life and death of a cell, *i.e.* the Bcl-2/Bax ratio, are markers of an involvement of the mitochondrion in the apoptotic program triggered by **7** in our cell system. This hypothesis was further supported by the reduction of

mitochondrial membrane potential, as well as by the increase of caspase-9 activity. Hence, our findings indicate that the alteration of the intracellular redox state induced by **7** could represent an underlying mechanism for the activation of the mitochondrial apoptotic pathway in melanoma cells.

Chemoresistance is a typical hallmark of advanced melanomas. It has been reported that the aggressive nature of melanoma is related to an accumulation of mutations in several key proliferation-regulating mechanisms, as well as in apoptosis-controlling pathways [48]. Defects in Akt expression occur in a significant proportion of malignant melanomas [49]. Under this concern, the early reduction of the pAkt protein levels caused by **7** was very interesting, because it has been demonstrated that CDC25B mediates the activation of Akt, probably through a dephosphorylation mechanism of specific protein kinases [50,51]. A key molecule involved in the regulation of cell cycle and apoptosis pathway is p53. Frequently, in melanoma this protein is not mutated, but its impaired functions depend on high levels of the phosphorylated form of MDM2, a typical inhibitor of p53 [52]. The time-dependent decrease of the basal level of p53 observed in both melanoma cell, and its higher level measured in treated cells mainly after a late incubation with **7**, suggest that this compound could affect the p53 protein stability. Indeed, higher levels of p53 in treated compared to untreated cells could be ascribable to a reduced activation of Akt, because this protein is responsible for the MDM2 phosphorylation [53,54]. On the other hand, it is likely that the reduced activation of Akt modulates the functions of other downstream proteins; under this concern, one possible candidate seems to be Bax, because of the increased levels of this pro-apoptotic factor observed upon treatment of A2058 with **7**. In conclusion, we suggest that the early reduction of pAkt levels could be related to a concomitant impairment of CDC25 functions. In turn, the reduced activation of Akt could cause the deregulation of other downstream pathways, leading to an increase of ROS level and later of p53 levels.

Hence, our data indicate that the anti-proliferative and pro-apoptotic effects triggered on melanoma cells after treatment with compound **7** is probably related to the inhibition potency exhibited by this molecule on the CDC25 phosphatase activity, as well as to the modulation of its

protein levels among the different forms. Therefore, the deregulation of CDC25 in melanoma cells suggests that this crucial element of cell cycle could be considered as a possible oncotarget *in vivo*. Under this concern, it is known that advanced anti-melanoma strategies are based on the usage of BRAF inhibitors, that selectively block the proliferation of melanoma cells harboring the BRAFV600E mutation [48]. However, the success of this therapy is not definitive, because usually the patients relapse because of acquired drug resistance, possibly due to the activation of others survival pathways. It has been observed that in many cases the anti-cancer therapies can induce the establishment of a pro-survival niche, allowing for therapeutic escape. In particular, melanoma cells readily adapt to nearly every pharmacological intervention and possess multiple routes to treatment escape. Loss of PTEN, a negative Akt regulator, as well as the increased Akt signalling, mediate a mesenchymal switch. In BRAFV600E/PTEN-null melanoma cell lines, vemurafenib is able to induce epithelial-to-mesenchymal transition (EMT). EMT is characterized by increased motility, upregulated expression of extracellular matrix factors, such as fibronectin (FN), and resistance to drug and apoptosis. Attachment to extracellular matrix has been identified as an important mechanism of drug resistance in a number of tumour systems. In melanoma cells, adhesion to FN prevents the induction of anoikis through increased PI3K signalling. The role of PI3K/Akt signalling in the adaptive responses that drive therapeutic escape was suggested by the finding that BRAF/PI3K inhibitor combination led to increased cytotoxicity [55].

An alternative strategy to reduce the therapeutic escape could be represented by the combination of two different drugs, cotargeting independent survival pathways that are critical for development and maintenance of melanoma. Hence, the study of the effects of CDC25 inhibitors in melanoma cells could be helpful for finding other molecular pathways, as possible targets for melanoma treatment. Future research will be devoted to the amelioration of the therapeutical potential of compound **7**; in particular, structural refinements will be performed to increase its inhibition power on CDC25, as well as the cytotoxic effects.

5. REFERENCES

1. Russell, P., Nurse, P. (1986) Cdc25+ functions as an inducer in the mitotic control of fission yeast. *Cell* **45**, 145–153.
2. Strausfeld, U., Labbé, J.C., Fesquet, D., Cavadore, J.C., Picard, A., Sadhu, K., Russell, P., Dorée, M. (1991) Dephosphorylation and activation of a p34cdc2/cyclin B complex *in vitro* by human CDC25 protein. *Nature* **351**, 242–245.
3. Karlsson-Rosenthal, C., Millar, J.B. (2006) Cdc25: mechanisms of checkpoint inhibition and recovery. (2006) *Trends Cell. Biol.* **16**, 285–292.
4. Terada, Y., Tatsuka, M., Jinno, S., Okayama, H. (1995) Requirement for tyrosine phosphorylation of Cdk4 in G1 arrest induced by ultraviolet irradiation. *Nature* **376** 358–362.
5. Iavarone, A., Massagué, J. (1997) Repression of the CDK activator Cdc25A and cell-cycle arrest by cytokine TGF-beta in cells lacking the CDK inhibitor p15. *Nature* **387**, 417–422.
6. Lindqvist, A., Rodríguez-Bravo, V., Medema, R.H. (2009) The decision to enter mitosis: feedback and redundancy in the mitotic entry network. *J. Cell. Biol.* **185**, 193–202.
7. Bartek, J., Lukas, J. (2001) Mammalian G1- and S-phase checkpoints in response to DNA damage. *Curr. Opin. Cell Biol.* **13**, 738–747.
8. Boutros, R., Lobjois, V., Ducommun, B. (2007) CDC25 phosphatases in cancer cells: key players? Good targets? *Nat. Rev. Cancer* **7**, 495–507.
9. Boutros, R., Dozier, C., Ducommun, B. (2006) The when and wheres of CDC25 phosphatases. *Curr. Opin. Cell Biol.* **18**, 185–191.
10. Aressy, B., Ducommun, B. (2008) Cell cycle control by the CDC25 phosphatases. *Anticancer Agents Med. Chem.* **8**, 818–824.
11. Dalvai, M., Mondesert, O., Bourdon, J.C., Ducommun, B., Dozier, C. (2011) Cdc25B is negatively regulated by p53 through Sp1 and NF-Y transcription factors. *Oncogene* **30**, 2282–2288.
12. St Clair, S., Giono, L., Varmeh-Ziaie, S., Resnick-Silverman, L., Liu, W.J., Padi, A., Dastidar, J., DaCosta, A., Mattia, M., Manfredi, J.J. (2004) DNA damage-induced downregulation of Cdc25C is mediated by p53 via two independent mechanisms: one involves direct binding to the cdc25C promoter. *Mol. Cell.* **16**, 725–736.
13. Kristjansdottir, K., Rudolph, J. (2004) Cdc25 phosphatases and cancer. *Chem. Biol.* **11**, 1043–1051.
14. Hernández, S., Bessa, X., Beà, S., Hernández, L., Nadal, A., Mallofré, C., Muntané, J., Castells, A., Fernández, P.L., Cardesa, A., Campo, E. (2001) Differential expression of cdc25 cell-cycle-activating phosphatases in human colorectal carcinoma. *Lab. Invest.* **81**, 465–473.
15. Wang, Z., Trope, C.G., Flørenes, V.A., Suo, Z., Nesland, J.M., Holm, R. (2010) Overexpression of CDC25B, CDC25C and phospho-CDC25C (Ser216) in vulvar squamous cell carcinomas are associated with malignant features and aggressive cancer phenotypes. *BMC Cancer* **10**, 233.

16. Lazo, J.S., Nemoto, K., Pestell, K.E., Cooley, K., Southwick, E.C., Mitchell, D.A., Furey, W., Gussio, R., Zaharevitz, D.W., Joo, B., Wipf, P. (2002) Identification of a potent and selective pharmacophore for Cdc25 dual specificity phosphatase inhibitors. *Mol. Pharmacol.* **61**, 720–728.
17. Park, H., Li, M., Choi, J., Cho, H., Ham, S.W. (2009) Structure-based virtual screening approach to identify novel classes of Cdc25B phosphatase inhibitors. *Bioorg. Med. Chem. Lett.* **19**, 4372–4375.
18. Pu, L., Amoscato, A.A., Bier, M.E., Lazo, J.S. (2002) Dual G1 and G2 phase inhibition by a novel, selective Cdc25 inhibitor 6-chloro-7-(2-morpholin-4-ylethylamino)-quinoline-5,8-dione. *J. Biol. Chem.* **277**, 46877–46885.
19. Kar, S., Lefterov, I.M., Wang, M., Lazo, J.S., Scott, C.N., Wilcox, C.S., Carr, B.I. (2003) Binding and inhibition of Cdc25 phosphatases by vitamin K analogues. *Biochemistry* **42**, 10490–10497.
20. Brisson, M., Nguyen, T., Wipf, P., Joo, B., Day, B.W., Skoko, J.S., Schreiber, E.M., Foster, C., Bansal, P., Lazo, J.S. (2005) Redox regulation of Cdc25B by cell-active quinolinediones. *Mol. Pharmacol.* **68**, 1810–1820.
21. Zhou, Y.B., Feng, X., Wang, L.N., Du, J.Q., Zhou, Y.Y., Yu, H.P., Zang, Y., Li, J.Y., Li, J. (2009) LGH00031, a novel ortho-quinonoid inhibitor of cell division cycle 25B, inhibits human cancer cells via ROS generation. *Acta Pharmacol. Sin.* **30**, 1359–1368.
22. Brezak, M.C., Quaranta, M., Contour-Galcerà, M.O., Lavergne, O., Mondesert, O., Auvray, P., Kasprzyk, P.G., Prevost, G.P., Ducommun, B. (2005) Inhibition of human tumor cell growth in vivo by an orally bioavailable inhibitor of CDC25 phosphatases. *Mol. Cancer Ther.* **4**, 1378–1387.
23. Brezak, M.C., Valette, A., Quaranta, M., Contour-Galcerà, M.O., Jullien, D., Lavergne, O., Frongia, C., Bigg, D., Kasprzyk, P.G., Prevost, G.P., Ducommun, B. (2009) IRC-083864, a novel bis quinone inhibitor of CDC25 phosphatases active against human cancer cells. *Int. J. Cancer* **124**, 1449–1456.
24. Lavecchia, A., Di Giovanni, C., Pesapane, A., Montuori, N., Ragno, P., Martucci, N.M., Masullo, M., De Vendittis, E., Novellino, E. (2012) Discovery of new inhibitors of Cdc25B dual specificity phosphatases by structure-based virtual screening. *J. Med. Chem.* **55**, 4142–4158.
25. Irwin, J.J., Sterling, T., Mysinger, M.M., Bolstad, E.S., Coleman, R.G. (2012) ZINC: a free tool to discover chemistry for biology. *J. Chem. Inf. Model* **52**, 1757–1768.
26. Lipinski, C.A. (2000) Drug-like properties and the causes of poor solubility and poor permeability. *J. Pharmacol. Toxicol. Methods* **44**, 235–249.
27. Romano, S., D'Angelillo, A., Pacelli, R., Staibano, S., De Luna, E., Bisogni, R., Eskelinen, E.L., Mascolo, M., Cali, G., Arra, C., Romano, M.F. (2010) Role of FK506-binding protein 51 in the control of apoptosis of irradiated melanoma cells. *Cell Death Differ.* **17**, 145–157.
28. Gelzo, M., Granato, G., Albano, F., Arcucci, A., Dello Russo, A., De Vendittis, E., Ruocco, M.R., Corso, G. (2014) Evaluation of cytotoxic effects of 7-dehydrocholesterol on melanoma cells. *Free Radic. Biol. Med.* **70**, 129–140.

29. Albano, F., Arcucci, A., Granato, G., Romano, S., Montagnani, S., De Vendittis, E., Ruocco, M.R. (2013) Markers of mitochondrial dysfunction during the diclofenac-induced apoptosis in melanoma cell lines. *Biochimie* **95**, 934–945.
30. Cecere, F., Iuliano A., Albano, F., Zappelli, C., Castellano, I., Grimaldi, P., Masullo, M., De Vendittis, E., Ruocco, M.R. (2010) Diclofenac-induced apoptosis in the neuroblastoma cell line SH-SY5Y: possible involvement of the mitochondrial superoxide dismutase. *J. Biomed. Biotechnol.* **2010**, 801726.
31. Bradford, M.M. (1976) A rapid and sensitive method for the quantitation of microgram quantities of protein utilizing the principle of protein-dye binding. *Anal. Biochem.* **72**, 248–254.
32. Frenzel, A., Grespi, F., Chmielewski, W., Villunger, A. (2009) Bcl2 family proteins in carcinogenesis and the treatment of cancer. *Apoptosis* **14**, 584–596.
33. Renault, T.T., Manon, S. (2011) Bax: addressed to kill. *Biochimie* **93**, 1379–1391.
34. Bellacosa, A., Kumar, C.C., Di Cristofano, A., Testa, J.R. (2005) Activation of Akt kinases in cancer: implications for therapeutic targeting. *Adv. Cancer Res.* **94**, 29–86.
35. Manning, B.D., Cantley, L.C. (2007) AKT/PKB signaling: navigating downstream. *Cell* **129**, 1261–1274.
36. Maddika, S., Ande, S.R., Panigrahi, S., Paranjothy, T., Weglarczyk, K., Zuse, A., Eshraghi, M., Manda, K.D., Wiechec, E., Los, M. (2007) Cell survival, cell death and cell cycle pathways are interconnected: implications for cancer therapy. *Drug Resist. Updat.* **10**, 13–29.
37. Clark, W.H.Jr, Elder, D.E., Guerry, D.4th, Epstein M.N., Greene, M.H., Van Horn, M. (1984) A study of tumor progression: the precursor lesions of superficial spreading and nodular melanoma. *Hum. Pathol.* **15**, 1147–1165.
38. Friedman, R.J., Heilman, E.R. (2002) The pathology of malignant melanoma. *Dermatol. Clin.* **20**, 659–676.
39. Lavecchia, A. (2015) Machine-learning approaches in drug discovery: methods and applications. *Drug Discov. Today* **20**, 318–331.
40. Lavecchia, A., Di Giovanni, C. (2013) Virtual screening strategies in drug discovery: a critical review. *Curr. Med. Chem.* **20**, 2839–2860.
41. Bales, E.S., Dietrich, C., Bandyopadhyay, D., Schwahn, D.J., Xu, W., Didenko, V., Leiss, P., Conrad, N., Pereira-Smith, O., Orengo, I., Medrano, E.E. (1999) High levels of expression of p27KIP1 and cyclin E in invasive primary malignant melanomas. *J. Invest. Dermatol.* **113**, 1039–1046.
42. Damia, G., Broggini, M. (2004) Cell cycle checkpoint proteins and cellular response to treatment by anticancer agents. *Cell Cycle* **3**, 46–50.
43. Gaul, L., Mandl-Weber, S., Baumann, P., Emmerich, B., Schmidmaier, R. (2008) Bendamustine induces G2 cell cycle arrest and apoptosis in myeloma cells: the role of ATM-Chk2-Cdc25A and ATM-p53-p21-pathways. *J. Cancer Res. Clin. Oncol.* **134**, 245–253.
44. Li, L., Zou, L. (2005) Sensing, signaling, and responding to DNA damage: organization of the checkpoint pathways in mammalian cells. *J. Cell. Biochem.* **94**, 298–306.

45. Monks, T.J., Hanzlik, R.P., Cohen, G.M., Ross, D., Graham, D.G. (1992) Quinone chemistry and toxicity. *Toxicol. Appl. Pharmacol.* **112**, 2–16.
46. Rudolph, J. (2005) Redox regulation of the Cdc25 phosphatases. *Antioxid. Redox Signal.* **7**, 761–767.
47. Zinkel, S., Gross, A., Yang, E. (2006) Bcl2 family in DNA damage and cell cycle control. *Cell Death Differ.* **13**, 1351–1359.
48. Gray-Schopfer, V., Wellbrock, C., Marais, R. (2007) Melanoma biology and new targeted therapy. *Nature* **445**, 851–857.
49. Robertson, G.P. (2005) Functional and therapeutic significance of Akt deregulation in malignant melanoma. *Cancer Metastasis Rev.* **24**, 273–285.
50. Chen, R.Q., Yang, Q.K., Lu, B.W., Yi, W., Cantin, G., Chen, Y.L., Fearn, C., Yates, J.R.3rd, Lee, J.D. (2009) CDC25B mediates rapamycin-induced oncogenic responses in cancer cells. *Cancer Res.* **69**, 2663–2668.
51. Liu, P., Begley, M., Michowski, W., Inuzuka, H., Ginzberg, M., Gao, D., Tsou, P., Gan, W., Papa, A., Kim, B.M., Wan, L., Singh, A., Zhai, B., Yuan, M., Wang, Z., Gygi, S.P., *et al.* (2014) Cell-cycle-regulated activation of Akt kinase by phosphorylation at its carboxyl terminus. *Nature* **508**, 541–545.
52. Lu, M., Breysens, H., Salter, V., Zhong, S., Hu, Y., Baer, C., Ratnayaka, I., Sullivan, A., Brown, N.R., Endicott, J., Knapp, S., Kessler, B.M., Middleton, M.R., Siebold, C., Jones, E.Y., Sviderskaya, E.V., *et al.* (2013) Restoring p53 function in human melanoma cells by inhibiting MDM2 and cyclin B1/CDK1-phosphorylated nuclear iASPP. *Cancer Cell* **23**, 618–633.
53. Mayo, L.D., Dixon, J.E., Durden, D.L., Tonks, N.K., Donner, D.B. (2002) PTEN protects p53 from Mdm2 and sensitizes cancer cells to chemotherapy. *J. Biol. Chem.* **277**, 5484–5489.
54. Feng, J., Tamaskovic, R., Yang, Z., Brazil, D.P., Merlo, A., Hess, D., Hemmings, B.A. Stabilization of Mdm2 via decreased ubiquitination is mediated by protein kinase B/Akt-dependent phosphorylation. *J. Biol. Chem.* **279**, 35510–35517.
55. Fedorenko, I.V., Abel, E.V., Fang, B., Wood, E.R., Chen, Y.A., Fisher, K.J., Iyengar, S., Dahlman, K.B., Wargo, J.A., Flaherty, K.T., Sosman, J.A., Sondak, V.K., Messina, J.L., Gibney, G.T., Smalley, K.S.M. (2016) Fibronectin induction abrogates the BRAF inhibitor response of BRAF V600E/PTEN-null melanoma cells. *Oncogene* **35**, 1225–1235.